Testing of a Multi-Stringer Post-Buckled Panel with Incremental Damage Detection

Jason Action[1]
Lockheed Martin, Marietta, GA

Upul Palliyaguru[2]
National Institute for Aviation Research, Wichita, KS

Wade Jackson[3], Joseph Zalameda[4]
NASA Langley Research Center, Hampton, VA, 23681

A multi-stringer panel was designed and tested to produce a failure mode of skin-stiffener delamination due to compression loading of a post-buckled skin to support the validation of high-fidelity progressive damage failure analysis modeling. The test procedure included multiple methods of data acquisition ranging from multiple strain gages, front and back digital image correlation, passive thermography, acoustic emission, and ultrasonic inspection to capture key events and damage progression prior to catastrophic failure. Detailed data showing the initial stiffness, onset of skin buckling, buckled mode shape, damage initiation load, damage propagation morphology, and peak load was captured. Two panel configurations were tested. The first had a Teflon insert placed in the interface between the skin and the stiffener flanges adjacent to the center skin bay. The second was subjected to impact damage to the skin-stiffener flange. In each case, continuously-loaded-to-failure tests were conducted first with passive thermography being used exclusively to determine key damage events. Then, incrementally loaded tests were completed where ultrasonic inspections were conducted between each increment. The amount of load applied between each increment was determined based on the in-situ damage detection provided by the passive thermography system. The results of the testing showed a complex delamination growth pattern which migrated between ply interfaces through matrix splits in the upper skin ply of the panel. The result of the testing produced very detailed data which will prove to be useful for validation of delamination growth and migration predictions from progressive damage failure analysis methods.

Nomenclature

PDFA	=	Progressive Damage Failure Analysis
ACP	=	Advanced Composite Program
V&V	=	Verification and Validation
FEM	=	Finite Element Model
CMM	=	Coordinate Measuring Machine
OML	=	Outer Mold Line
VCCT	=	Virtual Crack Closure Technique
DIC	=	Digital Image Correlation
AE	=	Acoustic Emission

1. Introduction

Advancements in computer technology have enabled analysts and designers of aircraft structure to incorporate difficult details and include damage progression methodologies into their analysis processes. Implementing a verified and validated method is key to obtaining an accurate solution for the structure being analyzed. The objective of the Progressive Damage and Failure Analysis (PDFA) team of NASA's Advanced Composite Program (ACP) is to develop improved PDFA methods that can reliably predict the onset and growth of damage in composite structures leading to their ultimate failure under both static and fatigue loading. Reliable methods can speed the design and certification process by allowing key design drivers to be assessed earlier in the design process, enabling a potential

---

[1] Aeronautical Engineer Staff, Advanced Development Programs, Associate Member
[2] Research Engineer, Nondestructive Evaluation Sciences Branch
[3]
[4] Research Engineer, Nondestructive Evaluation Sciences Branch

reduction in physical testing required while at the same time reducing the probability of later certification tests uncovering issues that would require costly redesigns.

The methods that the PDFA team are focused on during the ACP program would be subjected to a robust verification and validation (V&V) effort to address fundamental intralaminar, interlaminar, and interactions between interlaminar and intralaminar damage modes of composite structures. A part of the validation effort focused on a skin and stringer subcomponent that is representative in geometry and loading of an aircraft's wing or fuselage skin. The PDFA team chose a NASA developed plugin to an Abaqus finite element model (FEM) which implements a continuum damage methodology called CompDam [1].

To complete the validation of PDFA methods, a test configuration that captured the appropriate damage modes and progression of damage was necessary. A multi-stringer panel was designed where compression loads would first cause skin buckling, and the post-buckled response would lead to ultimate failure. The testing objective was to produce a failure mode between the stiffeners and the skin that would be a mixture of intralaminar and interlaminar damage without invoking other failure modes. Complex multi-system instrumentation combined with some pre-test modeling were used to capture all aspects of the test necessary for accurate V&V of the currently selected PDFA analysis tool as well as others in the future. The instrumentation captured the initial stiffness of the panel, onset of buckling load, buckled mode shape, post-buckled onset of damage, progression of damage prior to catastrophic failure, and peak load of the test.

2. Panel Configuration

A four-stringer hat stiffened test panel (Figure 1) was designed to generate a loading condition in which a crack might grow in the skin-stiffener interface. This crack growth would be achieved by first buckling the skin with compression loading. Additional compression loading beyond the skin buckling load amplifies the buckled shape of the skin and generates a pull-off loading condition between the hat and the skin at some locations along the length of the stiffeners. The skin was designed with 12 plies of IM7/8552 unidirectional tape in a quasi-isotropic layup so it would be relatively thin and exhibit a low instability load. A symmetric pad up region was added to the skin at the upper and lower loaded surfaces that doubled the thickness of the skin and followed the same quasi-isotropic layup. The pad up provided a stable boundary for the buckled skin and prevented an initial failure occurring next to the load application/reaction surfaces. The hat stiffeners were designed with 16 plies of IM7/8552 fabric. In the hat sidewalls and crown, the 16 fabric plies form a quasi-isotropic and balanced layup. The outer 12 plies of the hat's layup were extended outside of the hat section to form the attaching outer flanges. The edges of the outer flanges were designed such that they were at a 95°angle to the skin, instead of tapered. This generated a significant stress concentration at the hat flange to skin interface, which aided in generating damage that would be contained mostly at the hat-skin interface. The inner 4 plies of the hat's layup were wrapped around the inside of the hat section. This produced a largely continuous fabric (hat) to tape (skin) interface across the full width of the hat section. The hats were distributed across the panel such that width of the center skin bay was slightly wider than the outer bays. This produced a lower critical buckling load in the center bay than the outer skin bays, which focused the damage to occur in the flanges of the middle stiffeners that were adjacent to the center skin bay instead of randomly around the panel.

The panel was assembled in two configurations. In the first configuration, all stiffeners were located on the panel with pristine hat to skin interfaces. These panels were impacted to create a local disbond between the hat and the stiffener. The second configuration has a 0.25" wide Teflon strip placed in the hat to skin interface of the second and third hat stiffeners, on the flanges that are adjacent to the center skin bay, as shown in

Figure 2. The Teflon strip runs nearly the full length of the skin, terminating at 0.5” from the ramp to the pad up. The Teflon in the interface serves as the crack starter as the panel is loaded in compression. The skin and stiffeners in both configurations were co-cured to form the final assembled part.

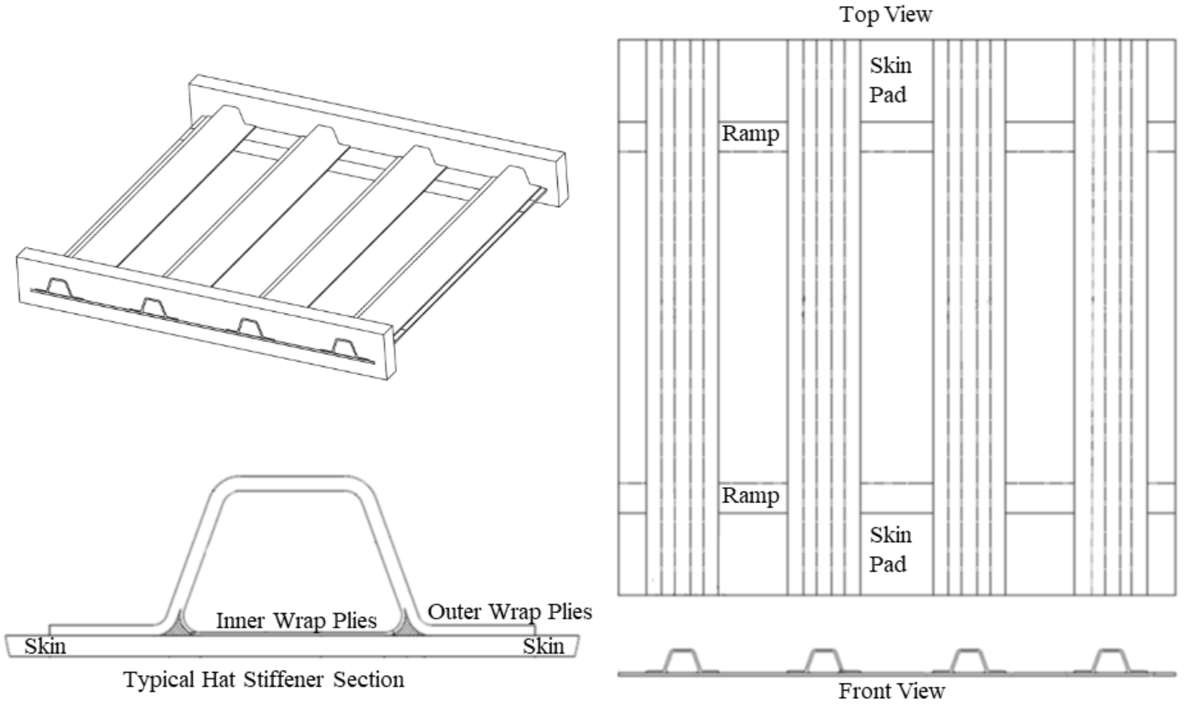

Figure 1: Multi-stringer hat stiffened panel

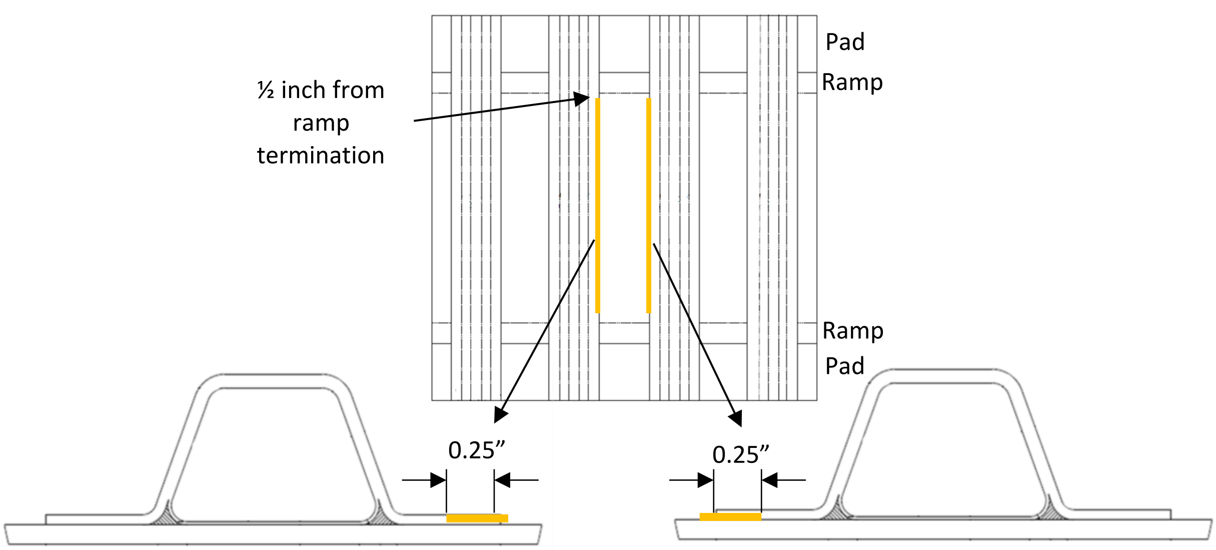

Figure 2: Multi-stringer panel with Teflon inserts

3. Fabrication and Pre-Test Activities

Ten multi-stringer panels were fabricated by Lockheed Martin in Fort Worth, Texas. Four of the panels were built with Teflon inserts between the skin and the stiffeners while the other six panels were built with no initial flaw to be impacted later. The final cured shape of each panel was measured using a coordinate measuring machine

(CMM). The CMM data revealed specific details of the panel's pre-test state after it was cured, as shown in Figure 3 for a representative case. It was found that the panels had a slight curvature due to the curing process in a cross section transverse to the stiffeners (section A-A) or parallel to the stiffeners (section 1-1). The amount of curvature that occurred transverse to the stiffeners was greater than the curvature that occurred parallel to the stiffeners by nearly a factor of 2. This curvature was consistent across the panel in both directions. The CMM cross-sections parallel to the stiffeners also revealed a manufacturing defect on the skin side of the panel. It was found that there was a joggle in the skin, on the OML side, in the ramp transition from the pad up to the nominal skin. This manufacturing defect was present in all 10 panels that were built.

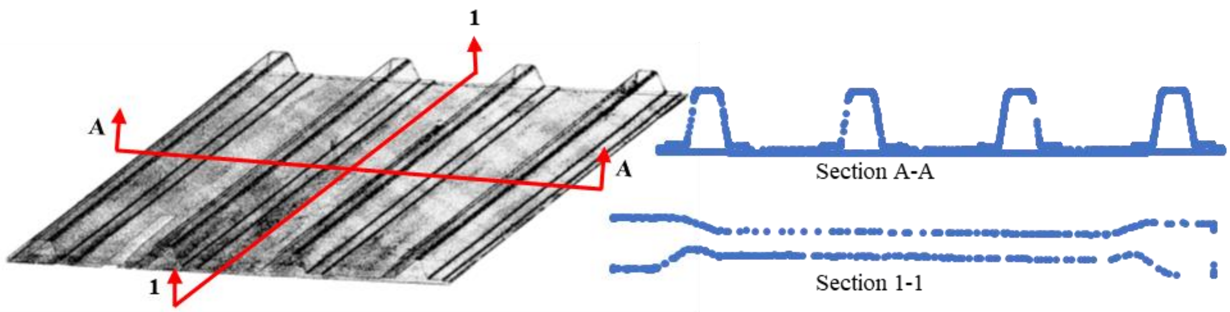

Figure 3: CMM results of a multi-stringer panel

All multi-stringer panels had potting added to the loaded ends of the panel. The potting was approximately 1" thick and provided a uniform loading surface when the panels were tested.

Three of the six panels that were manufactured without Teflon were impacted before static testing. The impact occurred on the skin side of the panel over the second stiffener flange that is adjacent to the center skin bay at the middle of the stiffener's length. An impact energy of approximately 5 ft-lb was used to generate a delamination as close to the skin-stiffener interface as possible without excessive damage to the skin. Figure 4 shows the ultrasonic inspection results and the delamination damage for each of the impacted panels. In each case, the delamination length along the free edge of the stiffener is between 0.96 inches and 1.34 inches long, and all have a width of approximately 0.25 inches. Most of the delamination damage occurred in the 1st ply interface with some damage occurring in the skin-stiffener interface. Evidence of through thickness matrix cracks in the 1st ply of the skin was also identified. There was no detectable damage through the remaining thickness of the skin and the impact left no deformation or visible evidence on the impact surface.

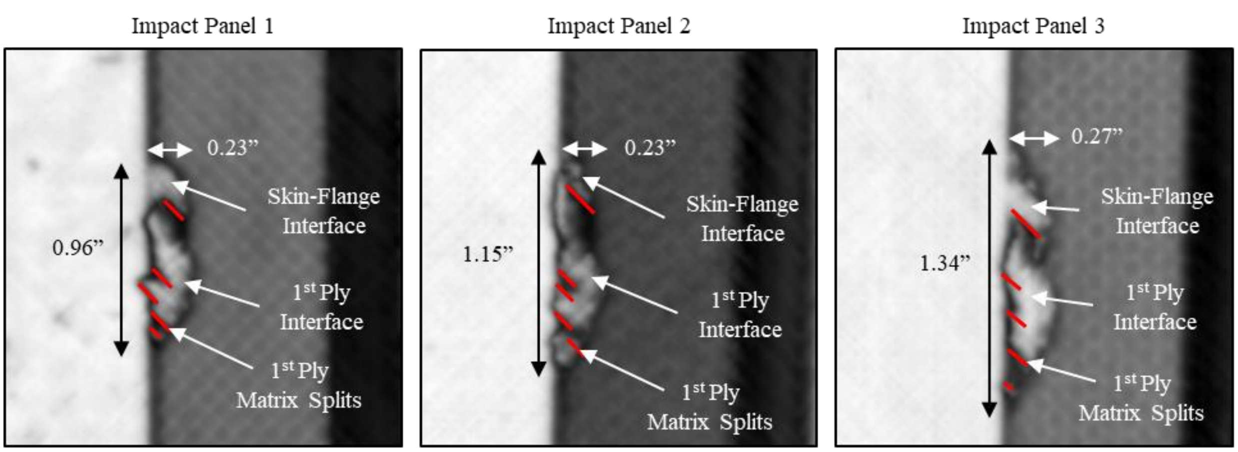

Figure 4: Impact damage for static testing of impacted multi-stringer panels

4. Prediction Model

Specific panel design decisions were made using engineering judgement and analysis, with the desired failure mode being stiffener separation due to crack growth. The finite element model shown in Figure 5 was created to perform the initial studies of the panel's design. The model was created using continuum shell elements for both the hat stiffeners and the skin, with the appropriate layup and material properties. The first and fourth hat stiffeners were tied to the skin while a virtual crack closure technique (VCCT) contact property was applied to the hat to skin interface on the second and third stiffeners [3]. Crack growth on the interface with the VCCT contact property was the only form of failure considered in the prediction model. The prediction model was built to replicate the panels with Teflon inserted in the hat to skin interface. The area of the Teflon insert was defined as the initially disbonded region required for the VCCT analysis. To bound the failure predictions, the panel was analyzed using a high value and a low value for the VCCT contact properties. The lower bound of the fracture toughness properties corresponded to a crack growing at a tape-tape interface, while the upper bound corresponded to a crack growing at a tape-fabric interface with a fully-developed resistance curve effect [3]. Basic boundary conditions were applied to mimic the test configuration, where the upper surface of the model was supplied an enforced displacement to generate a compression load. The lower surface reacted the applied load. The potting material on the ends of the test specimen was modeled as an out-of-plane restraint applied to the surface of the model in that area. The VCCT prediction model was analyzed using the implicit solver in Abaqus 2018 release FD03 and utilized the latest analysis parameters to enhance implicit solution stability during the crack growth analysis.

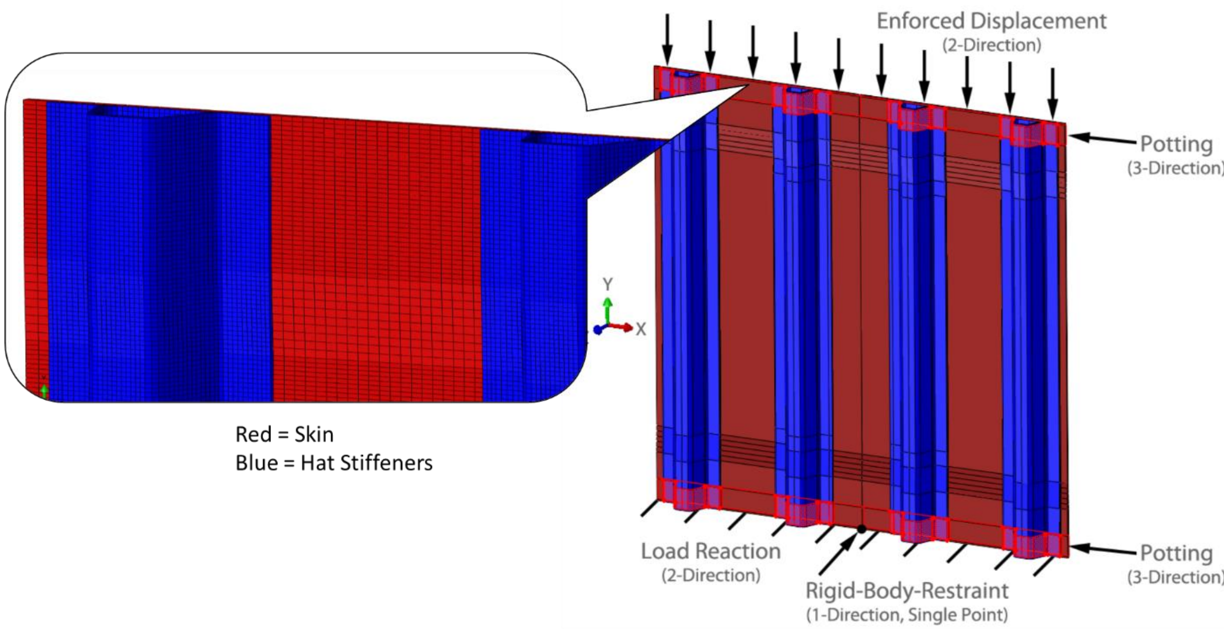

Figure 5: Multi-Stringer Hat-Stiffened Panel FEM

Figure 6 through Figure 8 show the prediction model results for the upper bound failure prediction that used tape-fabric propagation fracture toughness properties. The overall load-displacement predictions with upper and lower bounds of fracture toughness values are shown in Figure 6 along with key significant events. The analysis showed a linear response as load was initially applied to the model. It can be seen in the contour plot of **Figure 7** that the out-of-plane deflections in this initial load range (40 kip) produced a subtle bend to the panel that did not produce a buckled mode shape in the skin. The effects of the manufacturing defect at the ramp terminations can be seen at this load. Each of the skin bays exhibit an out-of-plane deflection behavior at the ramp terminations that causes a small area of the ramp to deflect into the stiffeners (red contour color) and a small area of the skin to deflect away from the stiffeners (blue contour color). Buckling of the center skin bay was shown to occur at an applied load of approximately 50 kip to 65 kip. The center skin bay entered a five-half-wave buckled mode shape where the center half-wave deflected away from the stiffeners. The contour plot at a load of 80 kip clearly shows that a buckled shape had fully developed in the center skin bay but has just begun to develop in the outer skin bays. As load continued to increase, the buckled shape took form in the outer bays. The plot of **Figure 7** shows the out-of-plane deflection vs. load for the center point of the panel. After the buckle of the center skin bay occurs, the deflection away from the stiffener of the center wave in the skin gains amplitude out to failure of the analysis. The buckled shape of the panel drove crack growth to occur under the 2nd and 3rd stiffeners local to the buckled waves that deflected away from the stiffeners. Figure 8 shows the crack growth prediction for the 2nd and 3rd stiffeners. The blue color indicates areas that the stiffeners are still attached to the skin, the orange indicates the inserted Teflon flaw, and the red region indicates the crack growth path at the end of the analysis. Within the crack growth region, the curved black lines are the boundaries of the crack growth solution at loads before the end of the analysis. The analysis concluded that the primary crack growth which would lead to the failure of the panel occurred adjacent to the center wave of the buckled skin and propagated transversely to the stiffener direction. This failure was a result of the skin buckling that occurred at a significantly lower load, then drove a peel mode in the skin-stiffener VCCT interface. The model predicted a failure range from 108 kip (tape-tape initiation fracture toughness properties) through 150 kip (tape-fabric propagation fracture toughness properties).

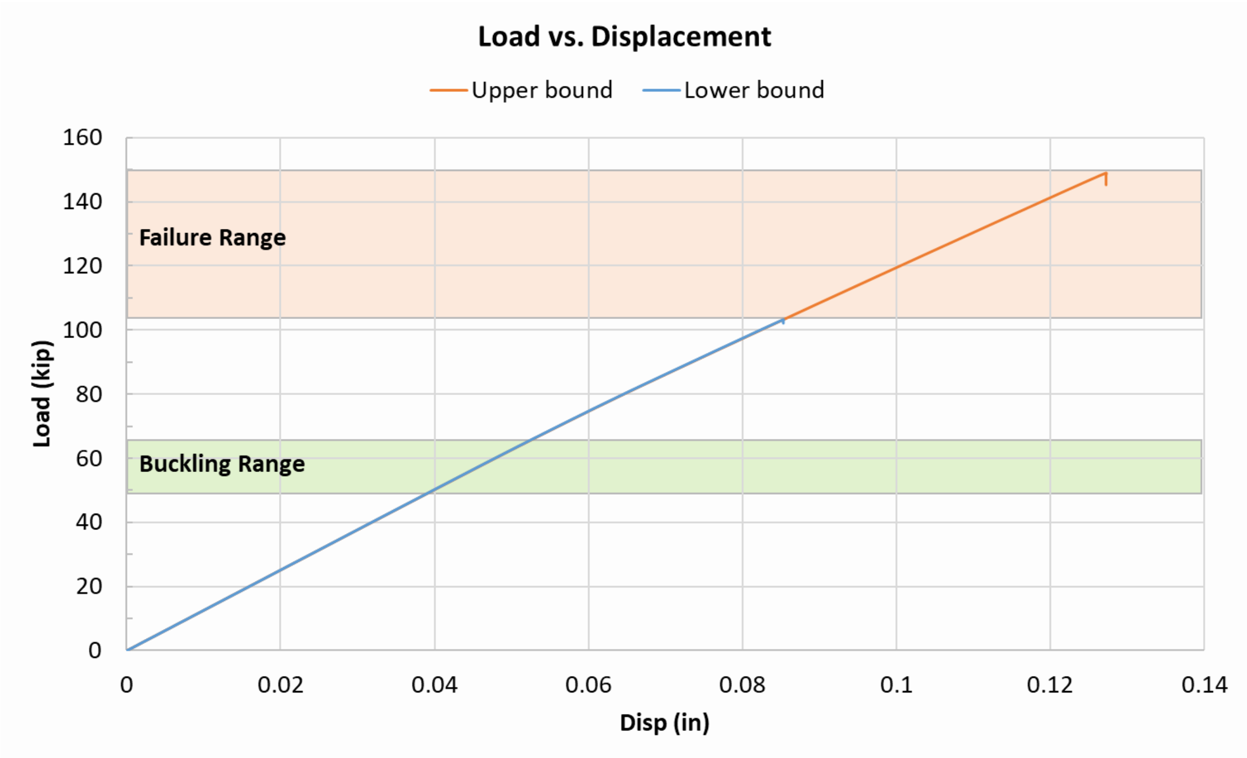

Figure 6: Panel Performance Predictions

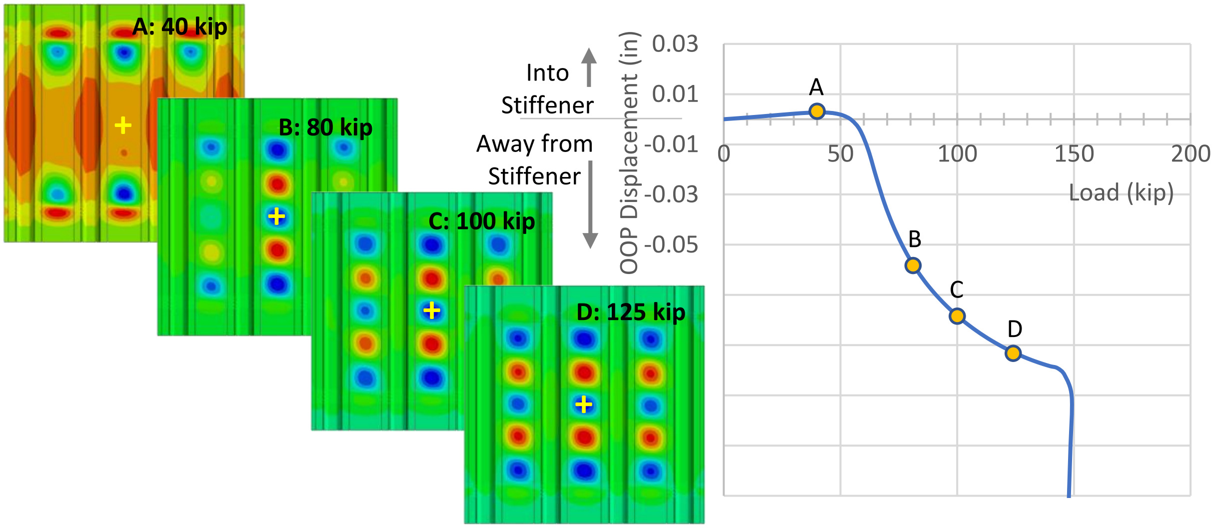

Figure 7: Finite element model results used for panel design

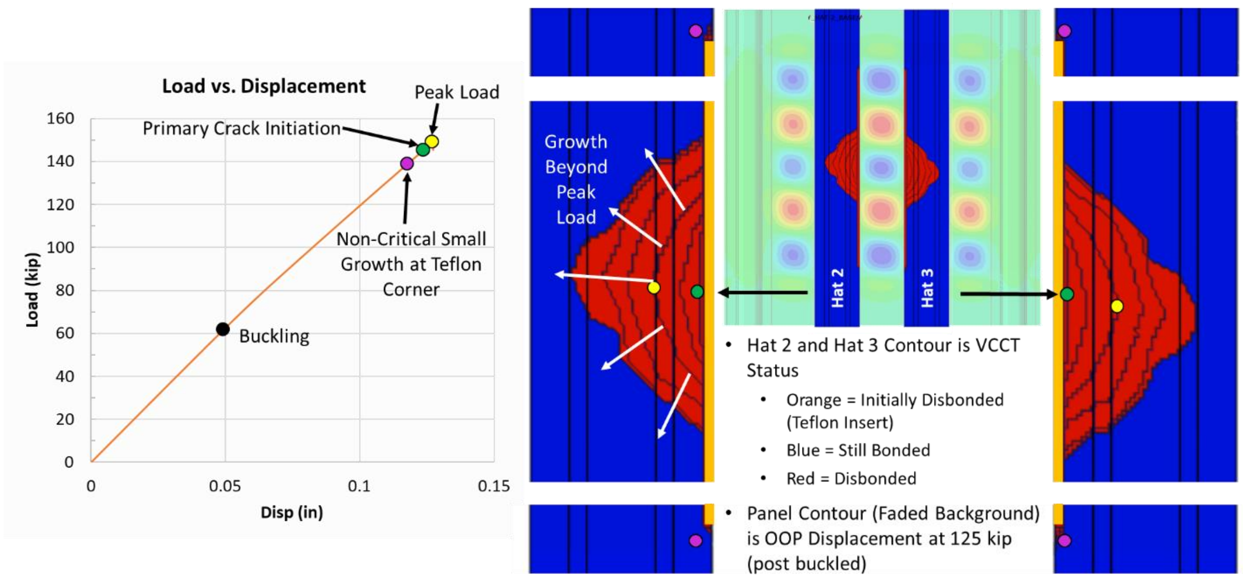

Figure 8: Prediction of crack growth from the Teflon Insert

The same modeling approach was used for the impacted panel. Figure 9 shows the updated VCCT contact properties for the impacted panel. The initially disbonded nodes of the 2nd stiffener to skin interface was updated to capture the approximate shape of the 0.13 in² delaminated area. A thin strip of nodes was also initially disbonded at the upper and lower regions of the 2nd stiffener to enable damage growth predictions due to the upper and lower buckled mode shapes. The initial crack length in the unimpacted areas was 0.02 inches. Only the 2nd hat stiffener flange was impacted, therefore, the 3rd hat stiffener interfacial property was given an initial delamination of only 0.02 inches deep, which spanned the full length of the stiffener.

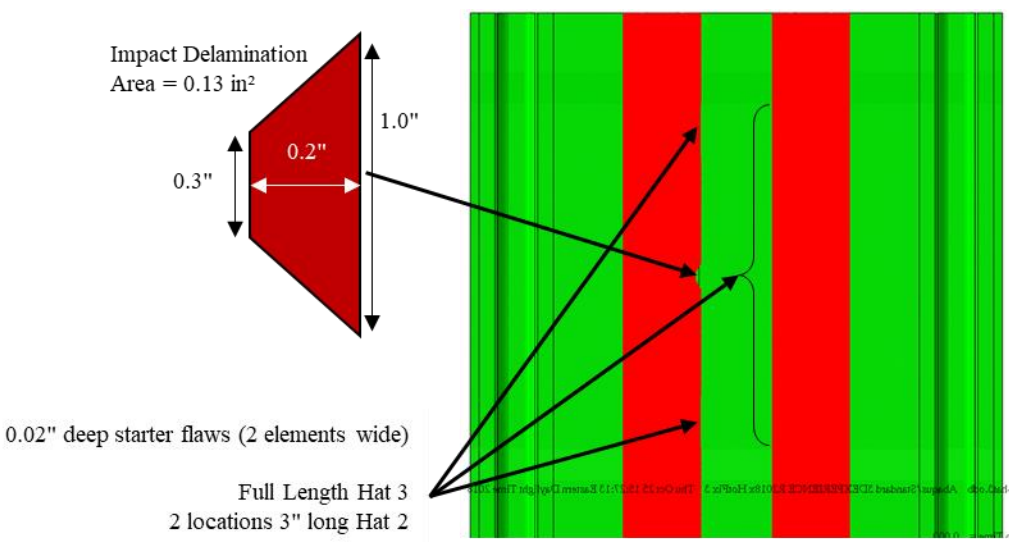

Figure 9: Impacted Panel Estimate

Because of similarities between the Teflon insert panels and the impacted panels, the global behavior of the analysis and the initial loading response was unchanged. The analysis was also completed only using the tape-tape interfacial properties in the VCCT contact surfaces. The analysis produced a peak load of 98 kip with the damage progression as shown in Figure 10. The crack growth initiated at approximately 87 kip and grew parallel to the stiffener. Growth between 87 kip and 97 kip continued in the longitudinal direction and produced a delaminated area that matched the buckled shape in the skin at that location. At 97 kip, the delamination damage grew transversely to the stiffener and maintained the same curved shape as the buckled skin. At the peak load of 98 kip, the impact delamination had significantly grown past the noodle of the 2nd stiffener and had initiated under the 3rd stiffener. This growth pattern continued beyond the peak load of 98 kip. The VCCT solution was also checked at the upper and lower peel zones of the model to see how close to damage onset these areas were. At peak load, the strain energy at these locations was less than half of the critical strain energy needed for crack growth to occur. Therefore, it was concluded that damage would not occur in these areas, and the critical damage growth would occur in the middle of the panel starting with the impact damage.

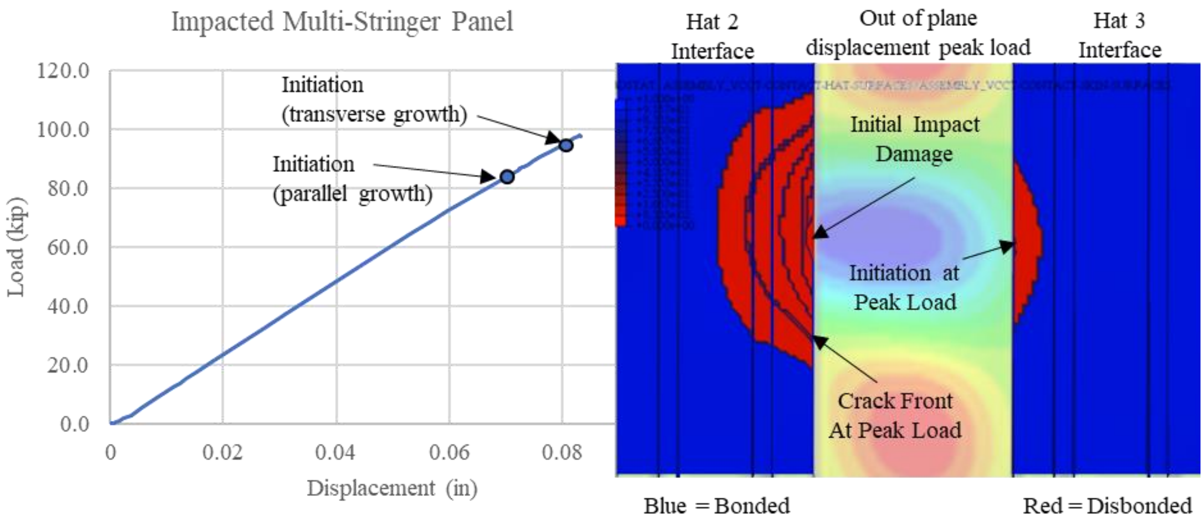

Figure 10: Impacted Panel VCCT results

5. Test Procedure

Static testing of the multi-stringer panels was completed by the National Institute for Aviation Research (NIAR). In all static tests (Teflon insert and impact damage), the same loading procedure, instrumentation, and data acquisition procedures were used. The instrumentation of all specimens is shown in Figure 11. Back-to-back axial strain gages were installed along the upper and lower edges of the panel at four skin locations (both outer edges and outer skin bays), the 2nd and 3rd stiffeners, and in the middle of the panel near the potting. Then, a speckle paint pattern was applied to both sides of the panel to enable the use of digital image correlation (DIC) during the test [4]. Finally, six acoustic emission (AE) sensors were applied to the crowns of the 2nd and 3rd stiffeners. A passive thermography system was also set up on the stiffener side of the specimen to provide in-situ damage monitoring during the test [5].

Each of the static specimens was installed in the test frame and loaded to approximately 30 kip, then the load frame head was leveled to ensure even loading of the panel. The output from the strain gages was evaluated to determine the orientation of the test specimen relative to the loading axis of the machine. After the panel alignment was completed, a final check was performed with a ramp to 80 kip. Then, the full test of the installed panel was executed. Load, stroke, and strain gage data were recorded at a rate of 100 Hz for the duration of the test. DIC images were captured at a rate of 1 Hz until the applied load reached approximately 80 kip, then the image capture rate was increased to 10 Hz. The passive thermography system captured filtered images of the test at a rate of 100 Hz and processed a time integration and subtraction technique to yield 4 images per second for in-situ damage monitoring. Two of the four Teflon insert panels and one of the three impacted panels were loaded continuously to failure to capture an overall behavior of the panel and determine the ability to detect in-situ damage. The remaining panels (two Teflon insert panels and two impacted panels) were incrementally loaded with ultrasonic inspection performed between the incremental stops of the test to capture the stable crack propagation that occurred between the stiffener and the skin prior to catastrophic failure of the panel. In each of the incrementally loaded tests, the load levels at which the ultrasonic inspections occurred was determined by the in-situ passive thermography monitoring, AE location results, and the intuition of the test engineers that were witnessing the tests.

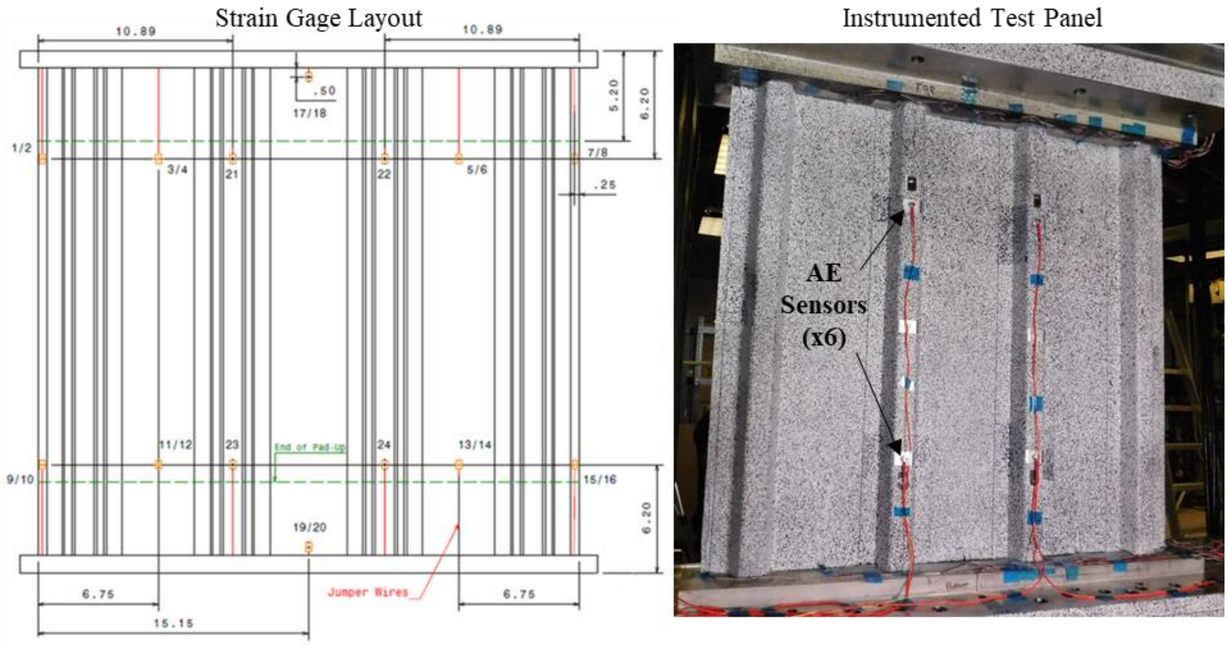

Figure 11: Instrumented multi-stringer test panel

6. Test Results

The results of the test panels with Teflon inserts were evaluated to determine the pre-buckled stiffness at the skin strain gage locations, the critical buckling loads of the center and outer skin bays, the buckled mode shapes of the skin bays, the onset of damage, the damage progression, and peak load. Figure 12 shows the average stiffness at each strain gage location as well as the strain gage output for the back-to-back gages at location 2. In general, it was found that the stiffness calculated at the free edges of the panel was higher than the outer skin bays. This was due to the proximity of the stiffener to the free edge. The output of the back to back strain gages showed very little to no bending that occurred at these locations and they also remained stable for the duration of the test. The back-to-back strain gages in the outer skin bays (location 2 strains seen in Figure 12) captured an initial bending in the panel due to the manufacturing defect found in the ramp termination on the skin side. To calculate the panel's stiffness in this area, the average strain was first determined. Then the stiffness was calculated based on the panel's behavior between 20 kip and 40 kip applied load to remove any other initial non-linearities that were present in the test data.

Figure 13 shows the out-of-plane displacements captured by the DIC system for the Teflon insert panel tests. The manufacturing defect at the ramp terminations caused a local out-of-plane displacement to occur in the skin in the pre-buckled load range. The center skin bay began to buckle into a five-half-wave mode shape at an average load of 44.6 kip. The mode shape was oriented such that the 1st, 3rd, and 5th half-waves deflected away from the stiffener and the 2nd and 4th half-waves deflected into the stiffener. A peel stress was generated at the stiffener flange termination adjacent to the three half-waves that deflected away from the stiffeners. The outer skin bays began to buckle into the same five-half-wave mode shape at an average load of 76.5 kip.

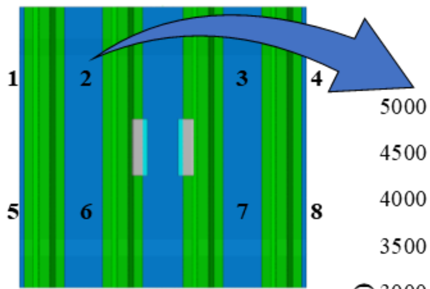

Test Average

Location	Stiffness
1	4.35 msi
2	3.84 msi
3	3.88 msi
4	4.32 msi
5	4.22 msi
6	3.62 msi
7	3.65 msi
8	4.27 msi

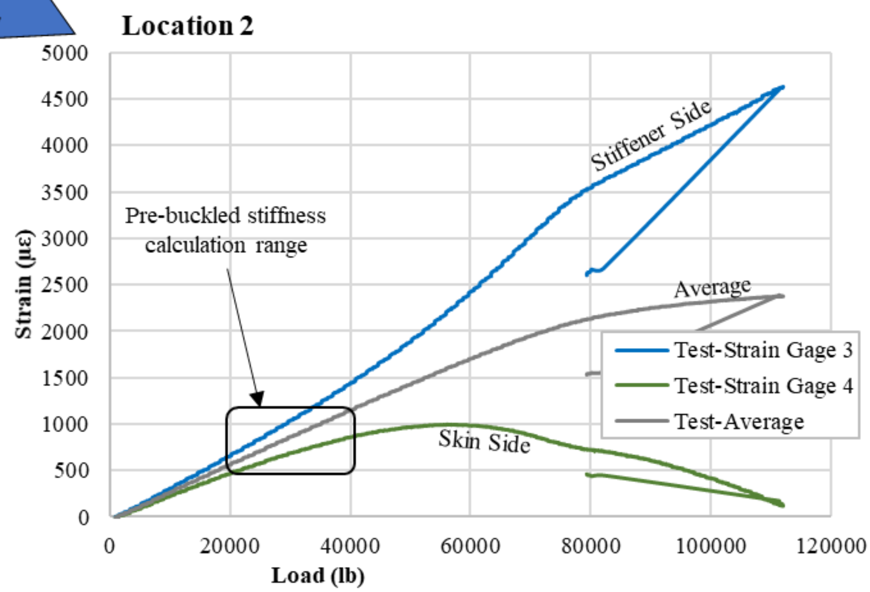

Figure 12: Sample strain gage output and stiffness calculation

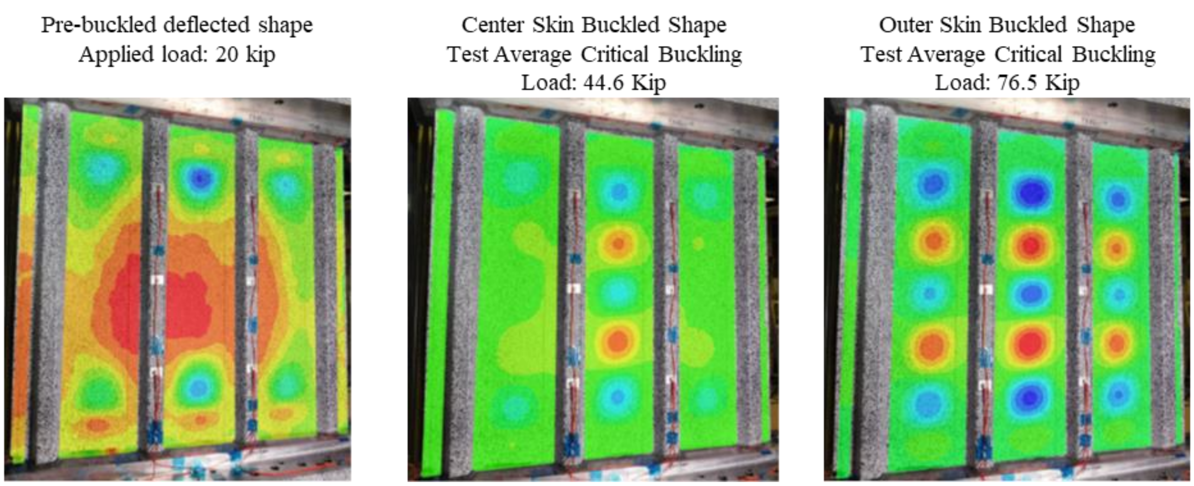

Figure 13: Out-of-plane DIC showing buckling shapes and critical buckling loads for a Teflon insert panel

Figure 14 shows the blended results of the passive thermography in-situ monitoring of a continuously loaded-to-failure test. It was seen that the initial damage growth occurred at the upper end of the Teflon insert at a load of 106.5 kip. Damage events at the center of the panel were then seen at 107 kip, followed by additional damage events captured at 107.7 kip. As the applied load reached 112 kip (peak load for test panel 2), the panel then suddenly failed. The in-situ passive thermography and the post-test inspections showed that the failure mode was delamination growth emanating from the center of the panel. The post-test passive thermography images were evaluated to identify the inspection loads for the incrementally loaded panels.

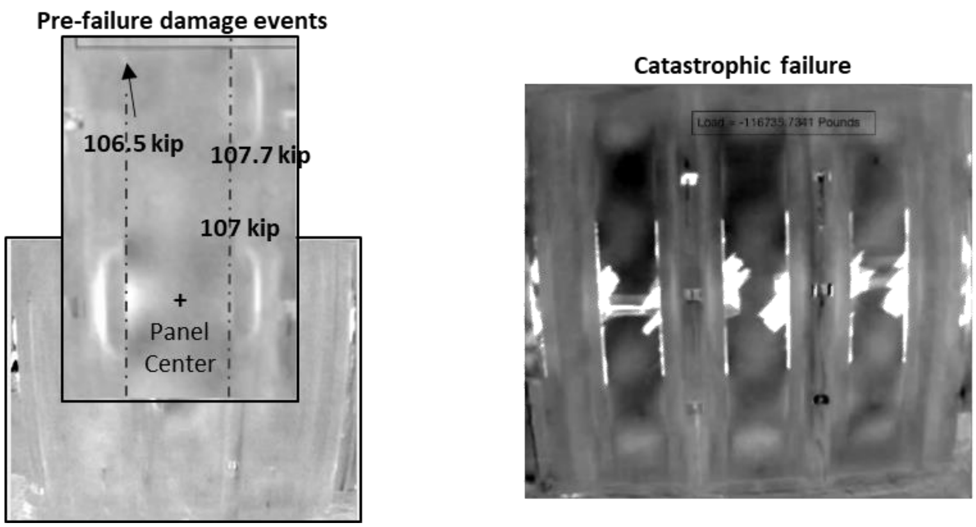

Figure 14: Passive thermography results from multi-stringer Teflon panel test 2, continuously loaded to failure

Figure 15 shows the inspection results from an incrementally loaded multi-stringer Teflon insert panel test. In the incrementally-loaded-to-failure testing, pre-peak load damage occurred at the end of the Teflon inserts as well as the center of the panel. The inspection focused on damage occurring in the center of the panel since this was the critical growth location which led to the catastrophic failure of the panel. At a damage initiation load of 106 kip, the ultrasonic inspection of this area revealed a rounded delamination under the stiffener flange that matched the center skin bay's buckled shape. The delamination occurred in both the skin-stiffener interface as well as the skin ply1-ply2 interface. Evidence of a matrix split in ply 1 could also be seen at the boundary between the skin-stiffener delamination and the skin ply1-ply2 delamination. The damage in the center of the panel continued to grow with additional load. Some growth was detected in the skin-stiffener interface; however, most of the growth occurred in the skin ply1-ply2 interface. Evidence of matrix splits could also be seen along the edge of the Teflon insert adjacent to the growth in the skin ply1-ply2 interface. None of these locations led to a significant migration of the delamination. One significant matrix split was present in the damaged area which largely separated the growth in the skin-stiffener interface from the growth in the skin ply1-ply2 interface. The damage morphology and progression were similar in both incrementally loaded tests. Only minor differences were found in local spots. For example, in one of the two incrementally loaded Teflon insert panel tests, a migration to the skin ply2-ply3 interface was detected near peak load (Figure 15).

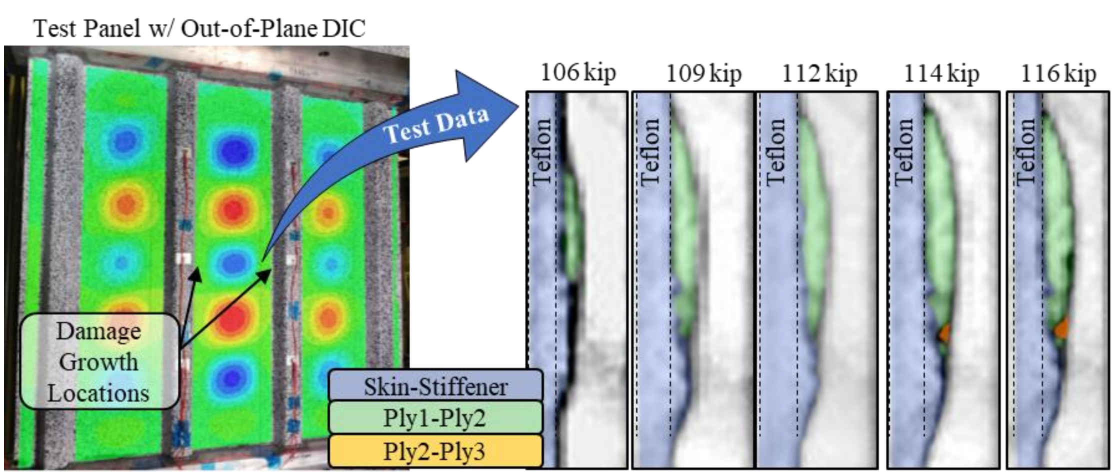

Figure 15: Ultrasonic inspection results from multi-stringer Teflon panel test 4, incrementally loaded to failure

Table 1 shows the peak load results from all four test panels with a Teflon insert flaw. An average peak load of 114 kip was calculated from the four Teflon insert tested panels. In general, the continuously loaded to failure panels yielded a lower peak load (112.15 kip average) when compared to the incrementally loaded to failure panels (116.5 kip average).

Table 1: Failure loads of Teflon insert multi-stringer panel tests

	Test Type	Peak Load
Teflon Test 1	Continuously Loaded	112.0 kip
Teflon Test 2	Continuously Loaded	112.3 kip
Teflon Test 3	Incrementally Loaded	116.1 kip
Teflon Test 4	Incrementally Loaded	116.9 kip

Average: 114.3 kip

Three impacted panels were also statically tested to failure. One of these was continuously loaded to failure to obtain the general panel response and pre-peak damage behavior while the other two were incrementally loaded to failure. The panel's pre-buckled stiffness, critical buckling loads, and buckled mode shapes were unaffected by the change in initial damage state of the inner stiffener flanges. The continuously loaded impacted panel test was conducted with the same test procedure as the continuously loaded Teflon insert panel, where the behaviors of the panel during the test were monitored to determine when damage events were going to occur relative to peak load of the panel. The continuously loaded panel reached a peak load of 117.9 kip, with the critical failure mode being a skin-stiffener separation emerging from the center skin buckle of the panel. The passive thermography system captured small damage events prior to failure of the panel, shown in Figure 16. The initial damage captured was at 100 kip applied load at the upper corner of the impact damage. Small damage growth events occurred mostly at the upper and lower corners of the damaged area at 102, 105.5, 112.5, and 116.6 kip, with a significant elliptical damage shape appearing at 112 kip. This damage sequence was used to anticipate when damage was going to occur in the incrementally loaded panel tests. Figure 17 shows the damage detected during one of the two incrementally loaded impact panel tests. The ultrasonic inspections show that the onset of damage was similar in load (105 kip) and consisted largely of growth in the skin ply1-ply2 interface, up to the overall impact damage perimeter. Scans were completed at 112 and 117 kip with very little additional growth. At 118 kip, a significant amount of growth occurred with delam growth in both the skin ply1-ply2 interface on the lower edges and the skin-stiffener interface on the upper edge. A significant matrix split had also opened at 118 kip which allowed the delamination migration to occur. A small amount of additional growth was encountered at 122 kip. Matrix splits in ply 2 of the skin began to appear at approximately 123 kip, which allowed a second migration of the delamination to the skin ply2-ply3 interface. A small amount of additional damage growth with the same characteristics was measured at 126 kip, just before failure of the panel. Table 2 shows the peak load results of all the statically tested impacted multi-stringer panels. An average peak load of 122.7 kips was achieved, with the incrementally loaded panels consistently failing at higher loads.

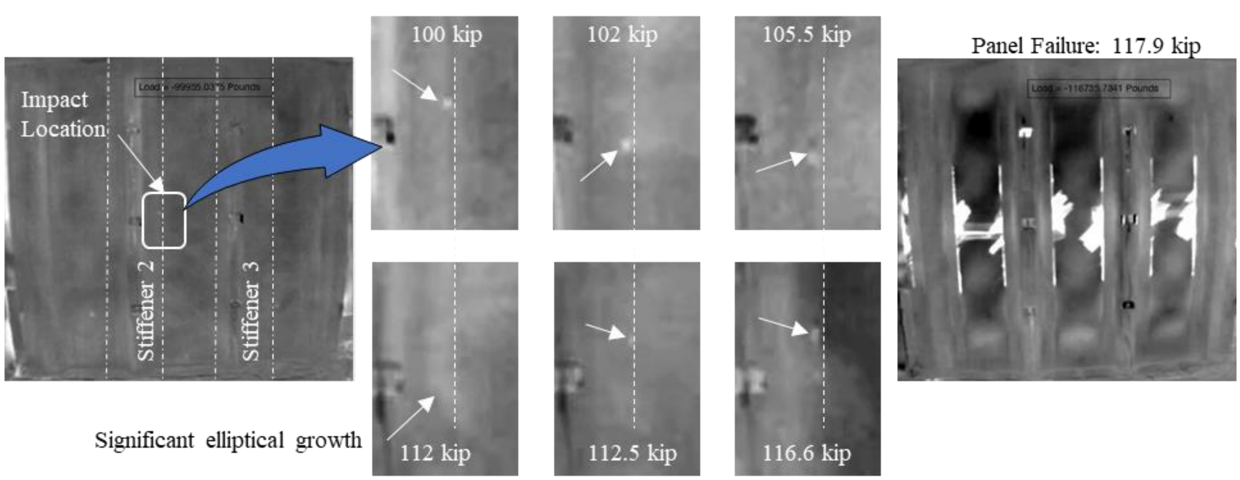

Figure 16: Passive thermography of impacted multi-stringer panel continuously loaded to failure

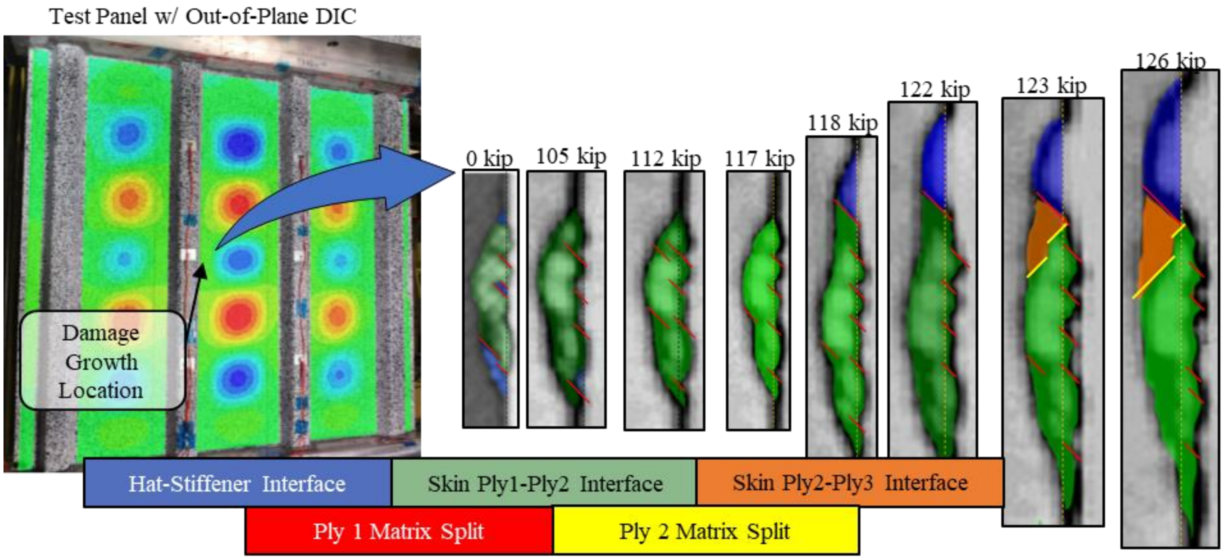

Figure 17: Ultrasonic inspection results from multi-stringer impact panel test 2, incrementally loaded to failure

Table 2: Failure loads of impacted multi-stringer panel tests

	Test Type	**Peak Load**
Impact Test 1	Continuously Loaded	117.9 kip
Impact Test 2	Incrementally Loaded	126.8 kip
Impact Test 3	Incrementally Loaded	123.3 kip
		Average: 122.7 kip

7. Analysis-Test Comparison

The predictive VCCT analysis results were very useful in guiding the test procedure and predicting the behaviors of the tested specimen. Figure 18 shows the overall panel response of the model and the test data. A reasonable comparison of strains at the strain gage locations was achieved. The initial panel deflections and buckled behavior of the center and outer skin bays of the panel performed as expected. The peak load of the tested panels correlated closely with the lower bound crack growth results of the analysis that were obtained with tape-tape fracture toughness interfacial properties. The VCCT crack growth results provided a decent representation to the damage found in the incremental inspections, as seen in Figure 19. The overall shape and growth directions were captured at the critical locations on the panel. The analysis underpredicted the initiation load by approximately 11 kip, and the crack front of the analysis obtained more of a rounded shape than the incremental testing showed. The analysis was also set up such that the crack growth occurred in only the stiffener-skin interface. Therefore, the matrix split in ply 1 and migration from the stiffener-skin interface to the ply1-ply2 interface of the skin was not captured.

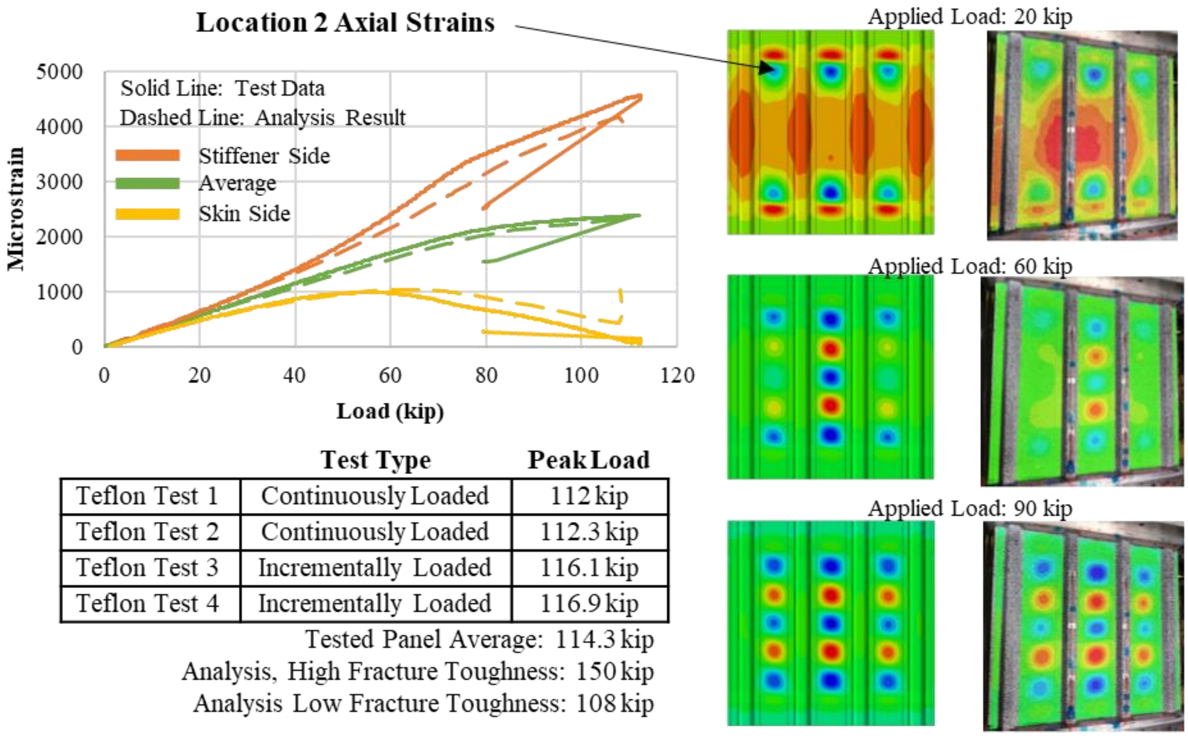

	Test Type	Peak Load
Teflon Test 1	Continuously Loaded	112 kip
Teflon Test 2	Continuously Loaded	112.3 kip
Teflon Test 3	Incrementally Loaded	116.1 kip
Teflon Test 4	Incrementally Loaded	116.9 kip

Figure 18: Panel response comparison of test data and predicted analysis results for a compression loaded multi-stringer panel with Teflon insert

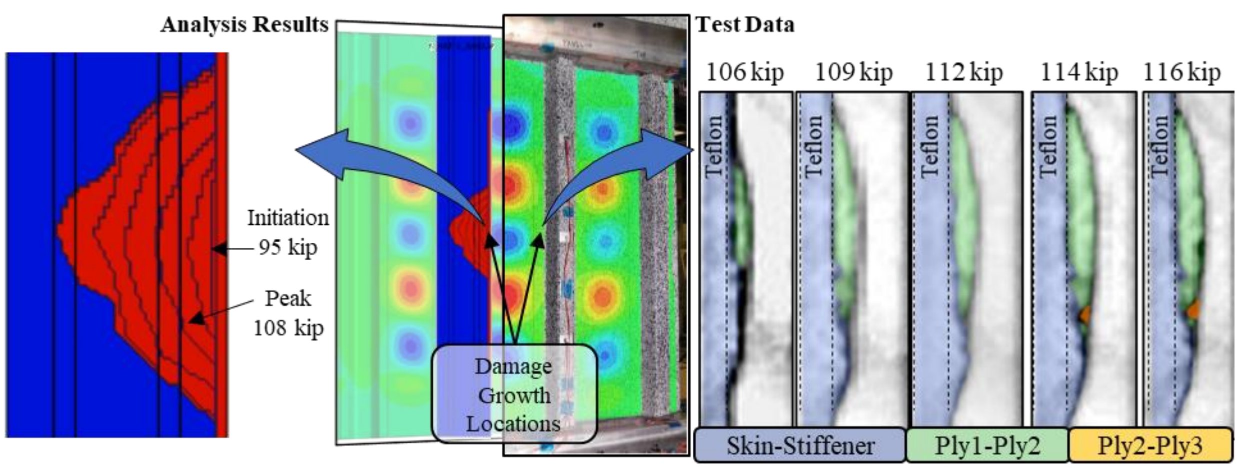

Figure 19: Damage progression comparison of test data and predicted analysis results for a compression loaded multi-stringer panel with Teflon insert

The overall response of the multi-stringer panel with impact damage was like the response seen for the Teflon insert panels for both the analysis and test data. The analysis was completed with only the tape-tape interfacial properties applied to the VCCT surfaces. Figure 20 shows the crack growth analysis results and test data for the multi-stringer panel with impact damage. The analysis showed a crack initiation load of 82 kip, a crack growth direction that was transverse to the stiffeners at 96 kip, and a peak load of 98 kip. Overall, the analysis captured the growth sequence and behavior, but the results were less accurate than the Teflon insert conditions. The analysis underpredicted the initiation and peak loads by more than 20 kip. The impact condition crack growth solution also exhibited characteristics similar to the Teflon insert case. A more rounded crack front was achieved, and the VCCT analysis was incapable of determining the matrix splits that occurred in the skin plies or the migration of the delamination between the skin ply1-ply2 interface and the skin-stiffener interface.

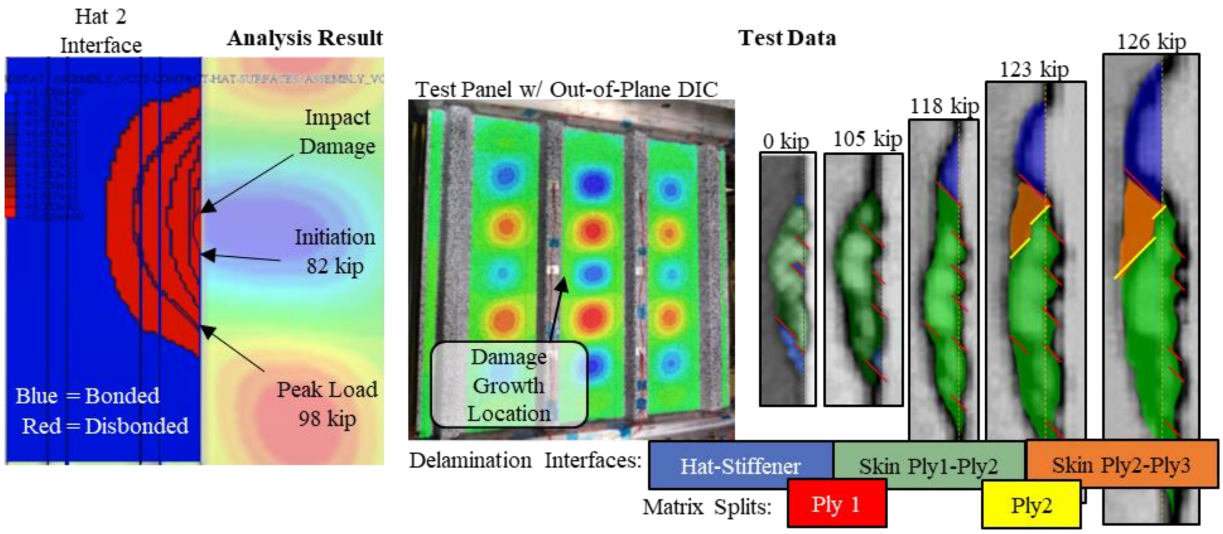

Figure 20: Damage progression comparison of test data and predicted analysis results for a compression loaded multi-stringer panel with impact damage

8. Conclusions

A pivotal aspect of validating a finite element analysis tool is having a good test condition to compare against. The multi-stringer panel in this study was designed with details that are representative of an in-service structural configuration, as well as features necessary to generate a stiffener separation failure mode during compression loading in the post-buckled regime. Initiation of stiffener separation and crack growth migration was the intended failure mode of the testing for validation of advanced finite element modeling techniques.

To generate the validation test data, an analysis model was used to characterize the behavior of the panel prior to the test and served as the basis to shape the test method. Advanced passive damage detection methods were used during the execution of the continuously loaded tests to determine appropriate stopping points to capture the delamination growth that occurred prior to the ultimate failure of the panel. Incremental testing was completed on four multi-stringer panels in total, two of them with Teflon inserts as the initial damage state and two of them with impact damage as the initial damage state. The incremental ultrasonic inspections revealed a damage growth pattern that was similar in both cases. In the Teflon insert multi-stringer panels, the delamination growth occurred in the skin-stiffener interface and the skin ply1-ply2 interface with a single significant matrix split joining the two. In the impacted panel condition, the initial damage also spanned the same ply interfaces. However, the initial delamination growth occurred only in the skin ply1-ply2 interface. When a significant amount of growth had occurred, the same damage pattern was found.

This multi-stringer configuration successfully produced test data that can be used in a validation effort for progressive damage finite element methods. Predictive VCCT models of the multi-stringer panel proved useful to anticipate the test response and provided a reasonable correlation to the test results but did not contain enough fidelity to capture all aspects of the failed panels. The analysis-aided test method produced repeatable initial stiffness, buckling loads, buckled mode shapes, damage onset, damage growth characteristics, and peak load data for panels with initial conditions of Teflon inserts and impact damage.

9. References

1. Rose, C. A., Davila, C. G., and Leone, F. A., “Analysis Methods for Progressive Damage of Composite Structures,” NASA/TM-2013-218024.
2. ABAQUS (2014), ABAQUS 6.14 Online Documentation. Retrieved 2019.
3. Foote, R. M. L., Mai, Y.-W., and Cotterell, B., "Crack Growth Resistance Curves in Strain Softening Materials," *Journal of the Mechanics and Physics of Solids*, Vol. 34, No. 6, pp. 593- 607, 1986.

4. Sutton, M. A., Orteu, J.-J., and Schreier, H. W., “Image Correlation for Shape, Motion and Deformation Measurements,” Springer 2009 edition, ISBN 978-0-387-78746-6.
5. Zalameda, J.N., Winfree, W.P, Seebo, J.P., and Johnston, P.H., “Thermography Inspection for Detection and Tracking of Composite Cylinder Damage During Load Testing,” AIP Conf. Proc. 1335, 2011, 450-457.